

## Uncertainty Quantification Applied to the Performance Analysis of a Conical Diffuser

E. Sauret<sup>1</sup>, R. Persky<sup>1</sup>, J.-C. Chassaing<sup>2</sup> and D. Lucor<sup>2</sup>

<sup>1</sup>School of Chemistry, Physics & Mechanical Engineering  
 Queensland University of Technology, Brisbane, Queensland 4000, Australia

<sup>2</sup>Sorbonne Universités, UPMC Univ Paris 06, CNRS, UMR7190, D'Alembert Institute, F-75005 Paris, France

### Abstract

This paper offers an uncertainty quantification (UQ) study applied to the performance analysis of the ERCOFTAC conical diffuser. A deterministic CFD solver is coupled with a non-statistical generalised Polynomial Chaos (gPC) representation based on a pseudo-spectral projection method. Such approach has the advantage to not require any modification of the CFD code for the propagation of random disturbances in the aerodynamic field. The stochastic results highlight the importance of the inlet velocity uncertainties on the pressure recovery both alone and when coupled with a second uncertain variable. From a theoretical point of view, we investigate the possibility to build our gPC representation on arbitrary grid, thus increasing the flexibility of the stochastic framework.

### Introduction

Diffusers play an important role in the design of turbine components as it helps recovering pressure and thus increasing the turbine efficiency. Conical diffusers have been extensively studied in the literature by means of Computational Fluid Dynamics (CFD). This is the case for the ERCOFTAC conical diffuser experimentally studied by Clausen [4, 5] and extensively investigated numerically [1, 2, 6–8]. These studies have highlighted the importance of several parameters such as the inlet swirl, turbulent kinetic energy and inlet velocity profiles, amongst the main uncertain parameters for the inlet boundary conditions. Also, as mentioned by Armfield et al. [1], the ERCOFTAC diffuser is an "extreme" case where the inlet rotational speed has been carefully adjusted to avoid any recirculation and separation of the flow. However, any small variations of inlet parameters can lead the numerical model to predict one or both of these regimes. Also, in real applications and especially in turbines, the input diffuser parameters are most likely to be uncertain because of the flow fluctuations coming from the rotor. The variability of these parameters may have dramatic effects on the global performance of the system. Thus, it is of particular importance to be able to quantify the impact of uncertain parameters by means of statistical analysis of the parameters of interest. Amongst the several different uncertain quantification methods available, the most widespread is the direct Monte-Carlo method. However, even if statistical approaches are straightforward to implement, they also have prohibitive computational costs. For that reason, a non-statistical generalised Polynomial Chaos (gPC) representation based on a pseudo-spectral projection method is adopted in this study [3]. Similar to Monte Carlo (MC) simulation, such approach doesn't require any modification of the CFD code.

In this work, a uniform distribution of the random parameters associated with Legendre polynomials is chosen. Due to the curse of dimensionality the uncertain parameters are investigated separately with high-order spectral projections while the combined effect of the parameters is initially investigated using low-order polynomials. The impact of the variable input parameters are evaluated on the pressure recovery of the diffuser. The stochastic space of each random variable is correlated to the range of uncertainty of the physical input parameters. Stochastic

results are analysed by means of density probability function of the pressure recovery and effectiveness of the diffuser. In particular, the sensitivity to uncertain parameters and their potential coupled effects on the stochastic aerodynamic field are discussed in details.

### Uncertainty Quantification Framework

#### Generalized Polynomial Chaos Method

In this work, the uncertainty quantification study relies on the generalised Polynomial Chaos (gPC) framework [9]. The gPC representation of a spatial random process  $u$  is

$$u(x, \Theta) = \sum_{\alpha \in \mathbb{N}^N} \hat{u}_\alpha(x) \phi_\alpha(\Theta), \quad (1)$$

where  $\Theta = \{\Theta_j(\omega)\}_{j=1}^N, N \in \mathbb{N}$ , is a  $\mathbb{R}^N$ -valued random array on a probability space  $(\Omega, \mathcal{A}, \mathcal{P})$  with probability distribution  $P_\Theta(d\theta)$  and  $d\theta$  is the Lebesgue measure.  $\phi_\alpha(\Theta)$  represent the multivariate orthogonal polynomials, with total degree not greater than  $P$ , that are built as tensor products of univariate orthogonal polynomials along each random dimension with respect to the probability measure  $P_\Theta(d\theta)$ . The deterministic coefficients in (1) are determined by:

$$\hat{u}_\alpha(x) = \mathbb{E}\{u(x, \Theta) \phi_\alpha(\Theta)\} / \mathbb{E}\{\phi_\alpha^2(\Theta)\}, \quad \text{for } \alpha \in \mathbb{N}^N, \quad (2)$$

where  $\mathbb{E}$  denotes the expectation. In practice, the order  $P$  of the polynomial basis is chosen based on accuracy requirements. The weights and nodes of the Gauss-Legendre quadrature are determined by solving an eigenvalue problem based on the Golub-Welsch algorithm.

#### Numerical Implementation

This nonintrusive approach has the advantage of not requiring modifications of the existing deterministic CFD solver. The evaluation of the unknown coefficients  $\hat{u}_\alpha(x)$  is equivalent to computing multidimensional integral using quadrature rules whose point locations and weights are dictated by the probability distribution of the inputs. In this study, we choose uniform distributions, giving the Legendre polynomials [10], as an appropriate basis with respect to the probability measure.

Two approaches are investigated to compute  $u(x, \Theta)$  at a given quadrature point  $x_q$ . First, we directly run the deterministic CFD solver for the values of the input random variable at  $x_q$ . In the second approach, we consider an arbitrary sampling of  $u(x, \Theta)$ , resulting for instance from a previously existing deterministic database. Next, we interpolate the CFD solution at  $x_q$  in order to perform the stochastic projection. This approach will be referred as interpolated CFD gPC (iCFD-gPC hereafter).

#### Test Case

The conical diffuser experimentally studied by Clausen [4, 5] is used in this study. The geometry is presented in figure 1. S0-S7 represent the locations of the experimental measurements.

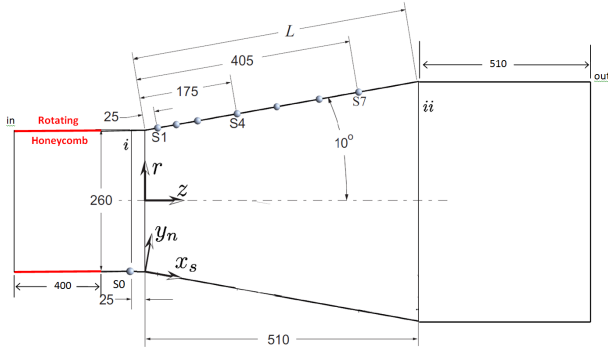


Figure 1. Non-scaled 2D schematic view of the ERCOFTAC conical diffuser with dimensions in [mm].

### Deterministic CFD Simulations

The open source code OpenFOAM is used to perform the deterministic CFD simulations. The 3D steady state flow solutions are computed with the *SimpleFOAM* solver using the standard high-Reynolds number  $k-\epsilon$  model with wall functions. The rotation of the honeycomb is set through the *addSwirlAndRotation* routine [2].

The present work builds upon previous studies from the OpenFOAM turbomachinery workgroup [7]. It was determined that Case 1 as presented by Nilsson [7] with an O-grid mesh gave adequate performance when compared to the experimental case and had a good  $y^+$  value using a moderate number of nodes. Mesh refinement was performed improving the  $y^+$  value of each section to an average of 20 which improved the comparison to the original experimental results of Clausen [4].

At the inlet of the computational domain, the velocity is purely axial and set to  $11.6 \text{ m}\cdot\text{s}^{-1}$ . The inlet turbulent kinetic energy is set to  $2.0184 \text{ m}^2\cdot\text{s}^{-2}$  and the turbulent energy dissipation to  $896.1 \text{ m}^2\cdot\text{s}^{-3}$  [2]. At the outlet the atmospheric pressure is set.

### Uncertain Parameters

Based on previous published works [1, 2, 6–8], five random disturbances in total, three freestream uncertain parameters and two geometric parameters are propagated using the gPC method detailed above: the inlet kinetic turbulence  $k$ , the inlet mean velocity  $U_\infty$ , the inlet swirl velocity  $W_\theta$ , the length of the diffuser  $L$  and the cone angle of the diffuser  $\alpha$ . The geometrical parameters and inlet swirl have been chosen because of their importance in the design of diffusers especially for pressure recovery, flow separation and recirculation concerns. Armfield et al. [1] also suggest that the experimental accuracy of the mean flow are within 6%. Furthermore, a wide range of values have been used in the previous numerical studies published [1, 2, 6–8].

A uniform distribution of the random parameters associated with Legendre polynomials is chosen in order to not favor any particular variable. The mean value  $\mu$  and the support of the distribution for each parameter are listed in table 1.

Combined uncertainty quantification is also performed for  $(k, U_\infty)$ ,  $(k, W_\theta)$ ,  $(U_\infty, W_\theta)$ ,  $(k, U_\infty, W_\theta)$ , and  $(L, \alpha)$ .

Uncertain Parameter	$\mu$	support
swirl velocity $W_\theta$ [rad. $\cdot$ s $^{-1}$ ]	52.65	[45–55]
turbulent kinetic energy $k$ [ $\text{m}^2\cdot\text{s}^{-2}$ ]	2.02	[0.1–10]
inlet mean velocity $U_\infty$ [ $\text{m}\cdot\text{s}^{-1}$ ]	11.6	[9–14]
half cone angle $\alpha$ [deg]	10	[8–12]
diffuser length $L$ [mm]	510	[410–610]

Table 1. Characteristics of the studied uncertain parameters: swirl velocity, turbulent kinetic energy, inlet mean velocity, half cone angle and diffuser length.

## Results

### Deterministic Aerodynamic Field and Response Surfaces

One important parameter to evaluate the effectiveness of the diffuser is the pressure recovery coefficient  $C_p$  ( $C_p = (p_{out} - p_\infty)/0.5\rho U_\infty^2$ ) as any improvements in the pressure recovery can increase the overall turbine efficiency.

Several factors such as separation and recirculation can dramatically affect the pressure recovery. Figure 2 shows the axial velocity field in the diffuser at the experimental conditions and for the lower and upper bounds as defined in table 1. At the experimental conditions, the simulations provide results close to the experimental data and we can note the absence of recirculation and separation in the diffuser. For the lowest inlet velocity ( $U_\infty=9.046 \text{ m}\cdot\text{s}^{-1}$ ), there is a large recirculation in the center of the diffuser near the exit while for the highest velocity ( $U_\infty=13.9539 \text{ m}\cdot\text{s}^{-1}$ ), there is no recirculation but a slight separation at the walls very close to the exit of the diffuser.

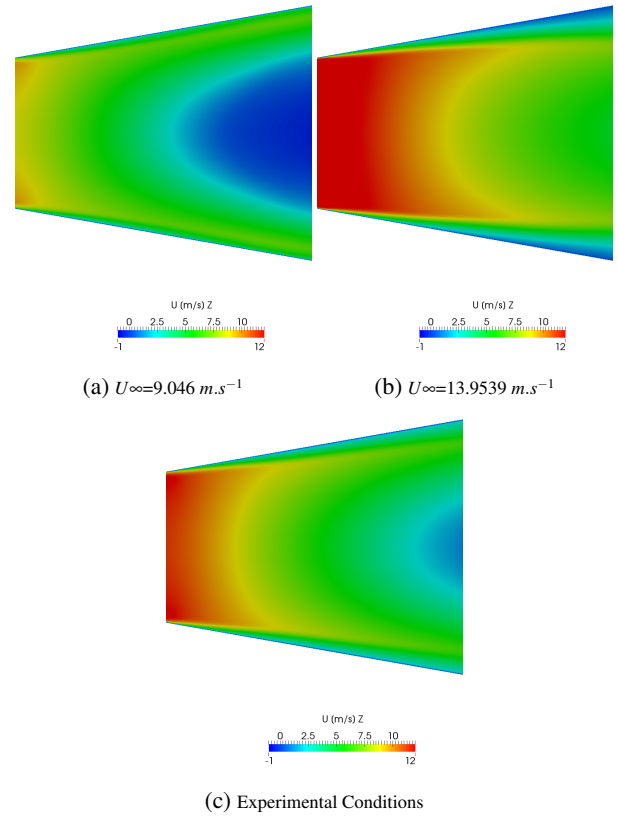


Figure 2. Axial velocity for (a) the lower ( $U_\infty=9.046 \text{ m}\cdot\text{s}^{-1}$ ) and (b) upper ( $U_\infty=13.9539 \text{ m}\cdot\text{s}^{-1}$ )  $U_\infty$  values and (c) for the experimental conditions using  $U_\infty$  as random parameter

Figure 3 shows the evolution of  $C_p$  with the five uncertain parameters  $U_\infty$ ,  $W_\theta$ ,  $k$ ,  $L$  and  $\alpha$ . It is clear that none of the uncertain parameters have a linear effect on the pressure recovery with, in some cases, relatively sharp gradients after or before the optimal  $C_p$  value. Thus these selected parameters are suitable for an uncertainty quantification investigation.

### Statistical Study

The mean and standard deviation for the gPC with 1 and 2 variables are presented in table 2. The gPC with one random variable is checked against the Monte-Carlo-based gPC method for which the polynomials are established from a MC draw.

Variable	gPC 1D (P=11)					gPC 2D (P=5)			
	$k$	$U_\infty$	$W_\theta$	$\alpha$	$L$	$U_\infty-k$	$W_\theta-k$	$W_\theta-U_\infty$	$\alpha-L$
$\mu$ (gPC)	0.797855	0.755063	0.789230	0.782003	0.779792	0.771833	0.802020	0.762643	0.776044
$\sigma \times 10^{-3}$ (gPC)	9.27099	49.0990	8.99946	8.01009	8.35796	4.61054	13.2119	39.6858	14.6711
CoV (gPC)	1.162	6.503	1.106	1.024	1.072	5.973	1.647	5.204	1.890
$\mu$ (gPC-MC)	0.797848	0.755034	0.789864	0.781996	0.779786	-	-	-	-
$\sigma \times 10^{-3}$ (gPC-MC)	9.26944	49.1173	8.73683	8.01942	8.36015	-	-	-	-

Table 2. Mean and standard deviation of the diffuser pressure recovery  $c_p$  for each individual uncertain parameter and coupled uncertain parameters with gPC and gPC-MC.

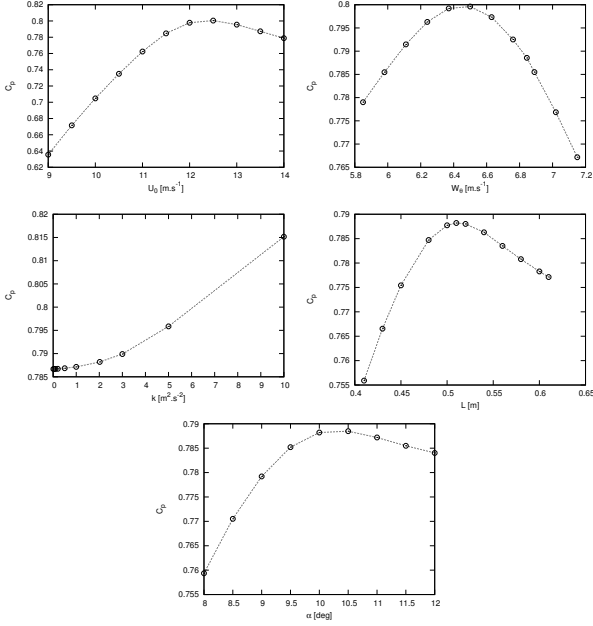


Figure 3. Initial deterministic solutions of  $C_p$  versus inlet velocity,  $U_\infty$ , swirl velocity  $W_\theta$ ,  $k$ ,  $L$  and  $\alpha$ .

While considering the effects of the input uncertainties individually on the pressure recovery, the lowest variability level is obtained for the cone angle  $\alpha$ , closely followed by the diffuser length  $L$  and the swirl velocity  $W_\theta$ . The inlet velocity  $U_\infty$  is the most influential parameter, followed by the inlet turbulent kinetic energy  $k$ . When parameters are coupled, the effect of  $U_\infty$  remains the most important with  $U_\infty-k$  and  $W_\theta-U_\infty$ , the most influential coupled random variables.

### Stochastic Recirculation Length

For each uncertain parameter, the mean value  $\mu$ , the standard deviation  $\sigma$  and the coefficient of variation  $\text{CoV}=\sigma/\mu$  of the recirculation length in the center of the diffuser was computed with the gPC at  $P=11$ . Table 3 shows that the longest recirculation in terms of mean value is obtained when varying  $U_\infty$ . The shortest length corresponds to the randomness in  $k$ . Table 3 also highlights that the sensitivity of the recirculation is much higher for  $k$  while  $U_\infty$  is far from the most influential uncertainty on the mean recirculation length.

Variable	$k$	$U_\infty$	$W_\theta$	$\alpha$	$L$
$\mu$	0.01166	0.21264	0.05669	0.17958	0.1894
$\sigma \times 10^{-3}$	72.2150	165.849	72.2150	91.1153	40.545
CoV	6.192	0.780	1.273	0.507	1.063

Table 3. Mean, standard deviation and CoV of the recirculation length for each individual random parameter using the gPC.

### Mean Velocity Profiles

The axial velocity profile at the S7 experimental location ( $x_s=405$  mm) near the diffuser exit obtained from the gPC using  $U_\infty$  as random variable is compared against the deterministic solution and experimental profile in figure 4. The deviation obtained from the gPC is also represented as an illustration of the range of possible realizations of the stochastic solution. We can note that the variance of  $U_x$  is more pronounced around the peak of velocity and near the center of the diffuser where the recirculation occurs. The plot also shows that this UQ is capable of capturing the experimental values until  $x_s=120$ mm. Beyond this value, the UQ still remains above the experimental values.

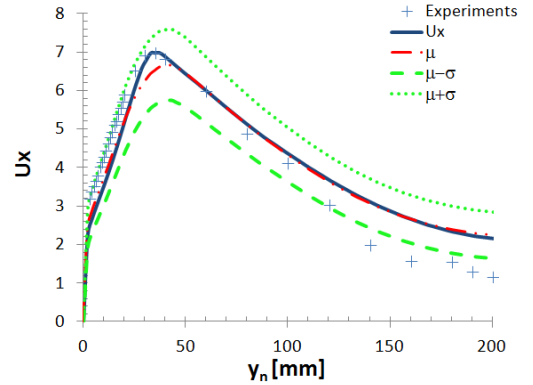


Figure 4. Axial velocity profile vs  $y_n$  at S7: comparisons between the experimental data [4], the deterministic solution and the mean and standard deviation obtained from the gPC method.

### Convergence Analysis

In this section, we investigate the accuracy and efficiency of the gPC and iCFD-gPC approaches by means of convergence analysis. The relative error of the variance of a typical quantity of interest is based on the best estimate obtained with  $P_{ref}=11$ :

$$err_{L_2}(\sigma_v^2) = \sqrt{\sigma_v^2(P) - \sigma_v^2(P_{ref})} \quad (3)$$

where  $P$  is the current  $P$ -order and  $v$  a typical random variable.

Figure 5 shows the CFD points of the iCFD-gPC and full gPC for  $P$  ranging from 1 to 11 when  $U_\infty$  is the random variable.

It is clear from figure 6 that the full gPC method achieves better convergence rate than iCFD-gPC based on a cubic interpolation scheme. On this figure, symbols represent our simulations while dashed lines are the corresponding linearly fitted decay rates. As expected, we can also note that for  $P$ -orders of the gPC below the interpolation order (here 3), the errors are similar for both methods. Beyond this order, the difference between both methods (gPC and iCFD-gPC) dramatically increases.

Figure 7 shows the corresponding deterministic solutions of  $c_p$  at the initial grid points and at the quadrature points and the

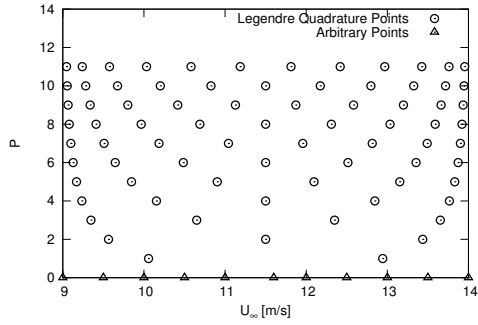


Figure 5. Legendre quadrature points and arbitrary support points for  $U_\infty$  for  $P = 1$  to 11

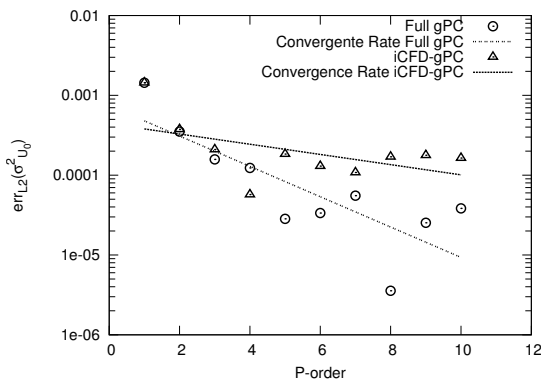


Figure 6. Convergence rates of the solution variance for the inlet mean velocity  $U_\infty$  vs  $P$ -order

interpolated CFD solutions. We clearly see the interpolation errors responsible for the poor convergence rate of the iCFD-gPC (figure 6), especially close to the highest values of  $c_p$ .

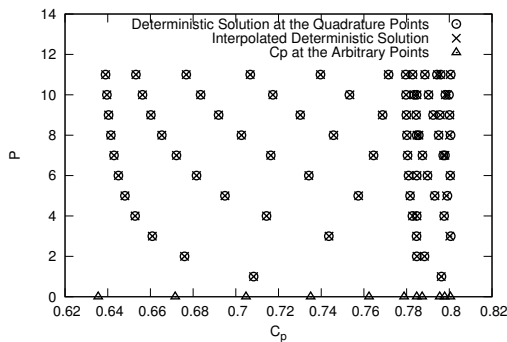


Figure 7. Deterministic solutions  $C_p$  for a variation of  $U_\infty$ , at the Legendre quadrature points, at the arbitrary points and interpolated from the arbitrary solutions for  $P = 1$  to 11.

## Conclusions

Uncertainty quantification is applied to the performance of a conical diffuser for the propagation of various aerodynamic and geometric uncertainties. This stochastic study highlights the importance of random variations in the inlet velocity over the other uncertainties (swirl, inlet turbulent kinetic energy, diffuser length and cone angle) on the pressure recovery both alone and when coupled to a second uncertain variable. However, for the variance of the recirculation length, the most influential uncer-

tainty is the inlet turbulent kinetic energy. Due to the non-linear effects associated with the recirculation, the velocity profiles are more sensitive close to the center of the diffuser where the recirculation is located. However, the highest sensitivity is found around the peak of velocity in the boundary layer. In addition, an interpolated CFD based gPC procedure was developed to deal with arbitrary samples of the CFD computations. As expected, results show that low interpolation order can strongly affect the convergence rate of the stochastic spectral projection approach. An improved accuracy and convergence rate were obtained with a higher-order interpolation. However, differences in the variance of the pressure recovery coefficients ranges between 4.7% for  $U_\infty$  up to 10% for  $k$ . Further study will be devoted to the coupling of the gPC method with higher-order interpolation schemes.

## Acknowledgements

Dr. E. Sauret thanks the Australian Research Council (DE130101183) and the Australian Academy of Science for their financial support.

## References

- [1] Armfield, S. W., Cho, N.-H. and Fletcher, C. A. J., Predictions of turbulence of turbulent quantities swirling flows in conical diffusers, *AIAA Journal*, **28** (3), 1990, 453–460.
- [2] Bounous, O., Studies of the ercoftac conical diffuser with openfoam, Technical report, Research Report 2008:05, Department of Applied Mechanics, Chalmers University of Technology, Goteborg, Sweden, 2008.
- [3] Chassaing, J.-C. and Lucor, D., Stochastic investigation of flows about airfoils at transonic speeds, *AIAA Journal*, **48**, 2010, 938–950.
- [4] Clausen, P. D., Koh, S. G. and Wood, D. H., Measurements of a swirling turbulent boundary layer developing in a conical diffuser, *Experiments Thermal and Fluid Science*, **6**, 1993, 39–48.
- [5] Clausen, P. D. and Wood, D. H., Some measurements of turbulent swirling flow through an axisymmetric diffuser, in *Proceeding of Sixth Symposium on Turbulent Shear Flows*, editor F. J. Durst, et al., University Paul Sabatier, Toulouse, France, 1987.
- [6] Gyllenram, W. and Nilsson, H., Very Large Eddy Simulation of Draft Tube Flow, in *Proceedings of the 23rd IAHR Symposium, Yokohama, Japan, October, 2006*.
- [7] Nilsson, H., Page, M., Beaudoin, M., Gschaidner, B. and Jasak, H., The openfoam turbomachinery working group, and conclusions from the turbomachinery session of the third openfoam workshop, in *24th Symposium on Hydraulic Machinery and Systems, IAHR, October 27-31, Foz Do Iguassu, Brazil, 2008*.
- [8] Page, M., Giroux, A.-M. and Massé, B., Turbulent Swirling Flow Computation in a Conical Diffuser with Two Commercial Codes, in *Proceedings of the 4th Annual Conference of the CFD Society of Canada*, 1996.
- [9] Spanos, P. and Ghanem, R., Stochastic finite element expansion for random media, *ASCE Journal of Engineering Mechanics*, **115**, 1989, 1035–1053.
- [10] Xiu, D. and Karniadakis, G., The Wiener-Askey polynomial chaos for stochastic differential equations, *SIAM Journal on Scientific Computing*, **24**, 2002, 619–644.